Article

Event-Triggered Attitude-Orbit Coupled Fault-Tolerant Control for Multi-Spacecraft Formation

Tao Wang [1,2,*], **Yingchun Zhang** [1] **and Hongchen Jiao** [2]

1   School of Astronautics, Harbin Institute of Technology, Harbin 150001, China; zhang@hit.edu.cn
2   China Academy of Space Technology, Beijing 100094, China; jhccast@163.com
*   Correspondence: 15210004024@163.com

Abstract: In this paper, the attitude-orbit coupled control problem for multi-spacecraft formation with limited communication capability and actuator failure is investigated. For the purpose of solving this problem, an event-triggered attitude-orbit coupled fault-tolerant control strategy is proposed. First, an integrated nonlinear dynamic model including the coupling characteristics of the attitude and orbit is established based on the Kane equation. Second, the nonlinear dynamic model is linearized at the reference state to facilitate the controller design. Third, a dynamic event-triggered mechanism is designed and an event-triggered fault-tolerant control law is developed. The stability of closed-loop control systems can be ensured under the designed control law and a sufficient condition that Zeno's behavior can be avoided is presented. Finally, simulation results are given to show the effectiveness of the proposed control method.

Keywords: attitude-orbit control; fault-tolerant control; spacecraft formation; dynamic event-triggered mechanism; actuator failure

MSC: 37M05

1. Introduction

When a serious failure of the actuator occurs in a spacecraft's attitude and orbit control systems, the spacecraft will lose control, which may lead to the task not being able to be completed. To continue to complete the established on-orbit tasks or implement on-orbit maintenance, it is required that another spacecraft and the failed spacecraft form a stable formation configuration to achieve stable control of relative attitude and orbit to ensure measurement, communication, and on-orbit maintenance. To ensure the on-orbit reliability, reconfigure ability, and maintainability of the satellite formation, formation control has drawn more and more attention from engineers, experts, and scholars of actuator failure.

Gao et al. investigated the leader-following attitude-consensus problem for a class of nonlinear multi-spacecraft formation flying systems with actuator failure and saturation. Based on a directed communication topology rooted in the lead spacecraft, a new fault estimation and fault-tolerant control scheme wee proposed, which can ensure the attitude synchronization [1]. Zou et al. studied the robust attitude-cooperative control of a spacecraft formation flying with actuator failure and proposed a distributed adaptive fault-tolerant attitude cooperative control law, which did not require online fault identification and could ensure that a group of spacecrafts simultaneously track the same time-varying reference attitude [2]. In reference [3], a reconfigurable fault-tolerant control method for spacecraft formation based on an iterative learning algorithm was proposed, which achieved the accurate maintenance of the spacecraft formation configuration in the case of space disturbance and thruster failure. Zhang et al. designed a fast, non-singular terminal sliding-mode finite-time fault-tolerant controller for a spacecraft formation with some actuators that completely failed and realized the synchronous tracking control of the spacecraft formation attitude [4]. Li et al. proposed a centralized adaptive fuzzy

approximation design to solve the multi-satellite attitude-synchronization control problem in the case of actuator failure through a non-singular fast terminal sliding mode controller and information topology [5]. Reference [6] researched the problem of anti-jamming and fault-tolerant control for a double-satellite formation configuration and designed an observer-based anti-jamming and fault-tolerant linear quadratic regulator-control strategy to achieve a high-precision and stable orbit of a double-satellite formation in the case of actuator failure.

Although many related results have been reported in the literature, most of them have been carried out on the orbit control and attitude control of a spacecraft formation independently, and there are few types of research on attitude-orbit coupling control in the case of the simultaneous failure of the attitude and orbital actuators. According to the constraints of spacecraft rendezvous and docking, unknown actuator faults, and unknown external disturbances, Sun proposed a relative pose adaptive fault-tolerant control method based on nonlinear feedback technology, with which the attitude-orbit coupling control of the spacecraft formation was realized [7]. Gui et al. proposed a new hybrid dual-quaternion integral sliding-mode control method, which solved the problem of simultaneous position and attitude tracking under the condition of actuator failures, and mass and inertia uncertainty. Then, the effectiveness of the method was verified through simulations [8]. In recent years, many scholars have carried out research on the attitude-orbit coupling control of spacecraft formations without considering actuator failure. Wang et al. proposed a state-feedback tracking-control law for relative position and attitude, which realized the attitude- and orbit-coordinated control of rigid microsatellite formations [9,10]. Successively, many scholars have proposed different control methods, such as the sliding-mode control method based on the master–slave control strategy [11–13], robust-control method based on a virtual structure [14,15], non-linear robust-control methods [16], and behavior-based finite-time control methods [17–19]. In recent years, dual quaternions have been widely used in the modeling of spacecraft formation dynamics [20]. At the same time, some scholars have adopted other modeling methods in view of the attitude-orbit coupling cooperative-control characteristics of multi-spacecraft formations. Huang et al. [21,22] established a generalized 6DOF dynamic model of non-contact internal forces using Kane equations and studied the relative balance of the electromagnetic formation of three spacecrafts.

Recently, with the rapid development in communication technology, networked control systems have been widely applied to spacecraft control systems. It should be pointed out that the traditional time-driven control strategy usually selects a smaller control period in order to ensure control performance under extreme conditions. However, a smaller control period will lead to a faster communication frequency, and a large amount of data is transmitted through the network. This will cause network congestion and some other unexpected phenomena, such as data transmission delay and packet loss. This leads to new parameter uncertainties and system performance will degrade. The event-triggered control scheme is an effective method that can reduce the communication rate and guarantee the performance of control systems simultaneously. Thus, based on the event-triggered control approach, networked control systems have been widely applied to spacecraft control systems. Combined with event triggering, research on the optimal control, adaptive control and other methods have been carried out [23,24]. Some of them have applied related methods to spacecraft attitude and orbit control systems [25–29], and demonstrated the effectiveness of the proposed control algorithm through theoretical analysis and simulation. However, most studies only consider the attitude control system or the orbit control system separately. There are relatively few studies on the attitude-orbit coupled 6DOF control system. Based on the above description, it is clear that the problem of event-triggered control for orbit-attitude coupling control systems has not been fully addressed, which motivated this study.

In this paper, the problem of attitude-orbit coupled control for multi-spacecraft formation with a limited communication capability and actuator failure are taken into account. An event-triggered attitude-orbit coupled fault-tolerant control strategy is proposed to

solve this problem. First, an integrated nonlinear dynamic model including the coupling characteristics of the attitude and the orbit is established based on the Kane equation. Second, the nonlinear dynamic model is linearized at the reference state to facilitate the controller design. In order to reduce the communication rate, the dynamic event-triggered mechanism is introduced. Finally, an event-triggered fault-tolerant control law is developed to overcome the influence of actuator failure and the event-triggered mechanism. The stability of closed-loop control systems is analyzed. A sufficient condition that guarantees that Zeno's behavior can be avoided is given. Simulation results are given to show the effectiveness of the proposed method. The advantages of the proposed method in this paper are twofold:

(1) In [16] and [22], the attitude controller and orbit controller were designed, respectively; while, in this paper, the integrated attitude and orbit controller are given since the motion of attitude and orbit is coupling. Thus, the proposed controller will have a better performance than the results of [16] and [22].

(2) In [25] and [28], the event-triggered mechanism is static, while in this paper, a dynamic event-triggered mechanism is proposed. Since some external variables are introduced in our dynamic event-triggered mechanism, the proposed dynamic event-triggered mechanism can be adaptively adjusted.

2. Attitude-Orbit Coupling Dynamics Modeling of Multi-Spacecraft Formations

2.1. Coordinate-System Definition

Define a formation system consisting of two controllable spacecrafts and one uncontrollable spacecraft, as shown in Figure 1. O_f is the mass center of the formation; ρ_1 and ρ_2 are the vector radii from O_f to the mass center of the controllable spacecraft 1 and 2, respectively; ρ_3 is the vector radii from O_f to the center of mass of the uncontrollable spacecraft; m_i is the mass of satellite i.
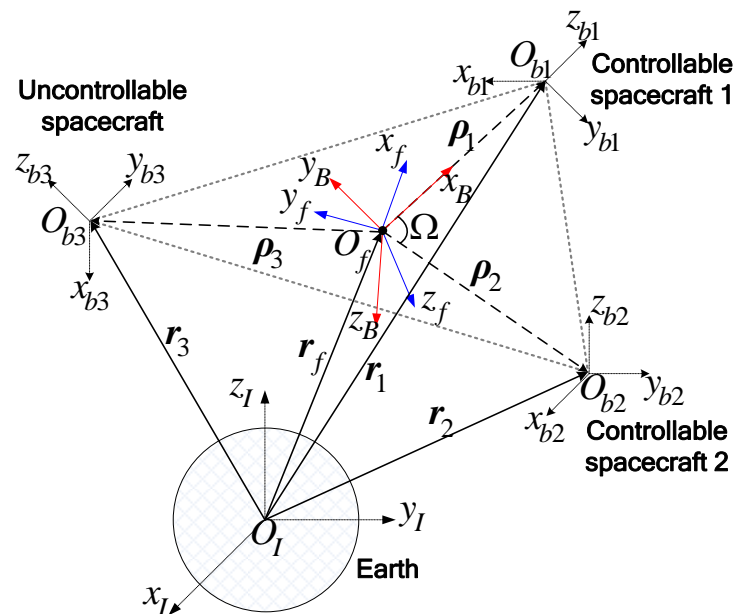
Figure 1. Formation system and reference coordinate system.

To facilitate the control-system design, the following coordinate systems are introduced:

(1)　Inertial coordinate system I: O_I is the mass center of the earth, the x_I axis points to the equinox, the z_I axis points to the north celestial pole, and the y_I axis satisfies the right-hand rule.

(2)　Orbital coordinate system H: O_f is the mass center of the formation, the x_f axis is along the radial vector direction of the formation center of mass in the coordinate system I,

the y_f axis points to the motion direction in the orbital plane, and the z_f axis points to the normal direction of the orbital plane, which satisfies the right-hand rule.

(3) Formation fixed coordinate system B: O_f is set as the origin, and the x_B axis points from the O_f to the mass center of spacecraft 1 O_{b1}. The y_B is in the plane defined by the mass centers of three spacecrafts and perpendicular to the x_B axis. The z_B axis is perpendicular to the plane determined by the mass centers of the three spacecrafts and satisfies the right-hand rule. The coordinate system B is obtained by rotating the coordinate system H by the φ, θ, and ψ angles in the order of 2-3-1.

(4) Satellite body coordinate system B_i: O_{bi} is the mass center of spacecraft i. Three coordinate axes are fixed to the spacecraft, and each axis is along the main axis of the inertia of the spacecraft. The coordinate system B_i is obtained by rotating the coordinate system B by the angles α_i, β_i, and γ_i in the order of 3-2-1.

2.2. System Dynamics Model

Assuming that the mass of the uncontrollable spacecraft is known while the inertia is unknown, sensors such as high-precision gyroscopes are working normally and the relative position (orbit/attitude) can be measured. However, the actuators are completely disabled and cannot generate the control force/torque. At the same time, controllable spacecraft 1, controllable spacecraft 2 and the uncontrollable spacecraft form a tight triangular formation (the distance between them is tens of meters). The mass center of the formation system runs in an approximately circular orbit, where the orbit radius is r_f. Here, $\boldsymbol{\rho}_1$, $\boldsymbol{\rho}_2$ and Ω are used to characterize the formation configuration. For the formation system, the system centroid satisfies $\sum_{i=1}^{3} m_i \boldsymbol{\rho}_i = 0$. As $\boldsymbol{\rho}_1$ and $\boldsymbol{\rho}_2$ are given, $\boldsymbol{\rho}_3$ can be determined as follows:

$$\begin{cases} \boldsymbol{\rho}_1 = \rho_1 x_B \\ \boldsymbol{\rho}_2 = \rho_2 \cos \Omega x_B - \rho_2 \sin \Omega y_B \\ \boldsymbol{\rho}_3 = (-m_1 \rho_1 / m_3 - m_2 \rho_2 \cos \Omega / m_3) x_B + m_2 \rho_2 \sin \Omega y_B / m_3 \end{cases} \tag{1}$$

The generalized coordinate $\boldsymbol{q}$ that defines the relationship between the formation configuration and the attitude can be expressed as:

$$\begin{aligned} \boldsymbol{q} &= \begin{bmatrix} q_1 & q_2 & q_3 & q_4 & q_5 & q_6 & q_{7,10,13} & q_{8,11,14} & q_{9,12,15} \end{bmatrix}^T \\ &= \begin{bmatrix} \rho_1 & \rho_2 & \phi & \varphi & \theta & \psi & \alpha_{1,2,3} & \beta_{1,2,3} & \gamma_{1,2,3} \end{bmatrix}^T \end{aligned} \tag{2}$$

Here, φ, θ, and ψ are the orientations of the formation relative to the orbital coordinate system H. In addition, α_i, β_i, and γ_i are the relative attitudes between the spacecrafts.

As the formation system runs in a circular orbit, the angular velocity of the coordinate system H relative to the coordinate system I is $\boldsymbol{\omega}^{H,I} = n z_f$, $n = \sqrt{\mu / r_{cm}^3}$.

The angular velocity of coordinate system B relative to coordinate system H, in coordinate system B, can be expressed as:

$$\boldsymbol{\omega}^{B,H} = \dot{\boldsymbol{\varphi}} + \dot{\boldsymbol{\theta}} + \dot{\boldsymbol{\psi}} = \begin{bmatrix} \dot{\psi} + \dot{\varphi} \sin \theta \\ \dot{\theta} \sin \psi + \dot{\varphi} \cos \theta \cos \psi \\ \dot{\theta} \cos \psi - \dot{\varphi} \cos \theta \sin \psi \end{bmatrix} \tag{3}$$

It can be known from the angular velocity superposition theorem that the angular velocity of coordinate system B relative to coordinate system I can be expressed as the sum of the angular velocity of coordinate system B relative to coordinate system H and the angular velocity of coordinate system H relative to coordinate system I, which can be written as:

$$\boldsymbol{\omega}^{B,I} = \boldsymbol{\omega}^{B,H} + C_{B,H} \cdot \boldsymbol{\omega}^{H,I} \tag{4}$$

Similarly, the angular velocity of coordinate system B_i relative to coordinate system B can be written in coordinate system B as:

$$\boldsymbol{\omega}^{B_i,B} = \dot{\boldsymbol{\gamma}}_i + \dot{\boldsymbol{\beta}}_i + \dot{\boldsymbol{\alpha}}_i = \begin{bmatrix} \dot{\beta}_i \sin\alpha_i - \dot{\gamma}_i \cos\alpha_i \cos\beta_i \\ -\dot{\beta}_i \cos\alpha_i - \dot{\gamma}_i \sin\alpha_i \cos\beta_i \\ -\dot{\alpha}_i + \dot{\gamma}_i \sin\beta_i \end{bmatrix} \tag{5}$$

Thus, the angular velocity of spacecraft i in the inertial system can be expressed as:

$$\boldsymbol{\omega}_i = \boldsymbol{\omega}^{B_i,I} = \boldsymbol{\omega}^{B_i,B} + \boldsymbol{\omega}^{B,I} \tag{6}$$

Based on the definition of angular velocity, the time derivative of the relative radius $\boldsymbol{\rho}_i$ of each spacecraft with respect to the inertial coordinate system can be calculated as

$$\boldsymbol{v}_i = \frac{^Id\boldsymbol{\rho}_i}{dt} = \frac{^Bd\boldsymbol{\rho}_i}{dt} + \boldsymbol{\omega}^{B,I} \times \boldsymbol{\rho}_i \tag{7}$$

The generalized rate $\boldsymbol{\eta}$ can be expressed as

$$\begin{aligned} \boldsymbol{\eta} &= \begin{bmatrix} \eta_1 & \eta_2 & \eta_3 & \eta_4 & \eta_5 & \eta_6 & \eta_{7,10,13} & \eta_{8,11,14} & \eta_{9,12,15} \end{bmatrix}^{\mathrm{T}} \\ &= \begin{bmatrix} \dot{\rho}_1 & \dot{\rho}_2 & \dot{\phi} & \omega_x^{B,I} & \omega_y^{B,I} & \omega_z^{B,I} & \omega_x^{B_{1,2,3},B} & \omega_y^{B_{1,2,3},B} & \omega_z^{B_{1,2,3},B} \end{bmatrix}^{\mathrm{T}} \end{aligned} \tag{8}$$

As $C_i = \cos q_i$, $S_i = \sin q_i$, and $T_i = \tan q_i$, the $\boldsymbol{\eta}$ can be reshaped as

$$\begin{bmatrix} \eta_1 \\ \eta_2 \\ \eta_3 \\ \eta_4 \\ \eta_5 \\ \eta_6 \\ \eta_7 \\ \eta_8 \\ \eta_9 \\ \eta_{10} \\ \eta_{11} \\ \eta_{12} \\ \eta_{13} \\ \eta_{14} \\ \eta_{15} \end{bmatrix} = \begin{bmatrix} \dot{q}_1 \\ \dot{q}_2 \\ \dot{q}_3 \\ \dot{q}_6 + \dot{q}_4 S_5 - n S_4 C_5 \\ \dot{q}_5 S_6 + \dot{q}_4 C_5 C_6 + n(C_4 S_6 + S_4 S_5 C_6) \\ \dot{q}_5 C_6 - \dot{q}_4 C_5 S_6 + n(C_4 C_6 - S_4 S_5 S_6) \\ \dot{q}_8 S_7 - \dot{q}_9 C_7 C_8 \\ -\dot{q}_8 C_7 - \dot{q}_9 S_7 C_8 \\ -\dot{q}_7 + \dot{q}_9 S_8 \\ \dot{q}_{11} S_{10} - \dot{q}_{12} C_{10} C_{11} \\ -\dot{q}_{11} C_{10} - \dot{q}_{12} S_{10} C_{11} \\ -\dot{q}_{10} + \dot{q}_{12} S_{11} \\ \dot{q}_{14} S_{13} - \dot{q}_{15} C_{13} C_{14} \\ -\dot{q}_{14} C_{13} - \dot{q}_{15} S_{13} C_{14} \\ -\dot{q}_{13} + \dot{q}_{15} S_{14} \end{bmatrix} \tag{9}$$

The velocity $\boldsymbol{v}_i$ and angular velocity $\boldsymbol{\omega}_i$ of each spacecraft are expressed in the form of $\boldsymbol{q}$ and $\boldsymbol{\eta}$, and by calculating the partial derivatives of $\boldsymbol{v}_i$ and $\boldsymbol{\omega}_i$ with respect to $\eta_r (r = 1, \cdots, 15)$, the partial derivatives of the velocity and angular velocity ($\boldsymbol{v}_r^i$ and $\boldsymbol{\omega}_r^i$) of spacecraft i can be obtained, respectively.

The generalized inertial force F_r^* and the generalized active force F_r can be calculated as follows:

$$\begin{cases} F_r^* = \sum\limits_{i=1}^{3} -m_i \boldsymbol{a}_i \cdot \boldsymbol{v}_r^i + \sum\limits_{i=1}^{2} -\left(\boldsymbol{J}_i \dot{\boldsymbol{\omega}}_i + \boldsymbol{\omega}_i \times \boldsymbol{J}_i \boldsymbol{\omega}_i\right) \cdot \boldsymbol{\omega}_r^i \\ F_r = \sum\limits_{i=1}^{3} \boldsymbol{R}_i \cdot \boldsymbol{v}_r^i + \sum\limits_{i=1}^{2} \boldsymbol{T}_i \cdot \boldsymbol{\omega}_r^i \end{cases} \tag{10}$$

Here, $\boldsymbol{a}_i$ is the acceleration of spacecraft i relative to the inertial coordinate system, and $\boldsymbol{J}_i$ is the rotational inertia of spacecraft i. $\boldsymbol{R}_i$ and $\boldsymbol{T}_i$ are the resultant external force and moment relative to the mass center of spacecraft i.

Considering the main inertia assumption, that is, the rotational inertia of each spacecraft satisfies $J_i = J_i \cdot E$, E is the unit matrix. Therefore, the generalized inertial force can be expressed as:

$$
\begin{aligned}
F_1^* &= m_1(a_{3x} - a_{1x}) \\
F_2^* &= m_2 C_3(a_{3x} - a_{2x}) - m_2 S_3(a_{3y} - a_{2y}) \\
F_3^* &= -m_2 q_2 C_3(a_{3y} - a_{2y}) - m_2 q_2 S_3(a_{3x} - a_{2x}) \\
F_4^* &= -m_2 q_2 S_3(a_{3z} - a_{2z}) - \left(T_{1x}^* + T_{2x}^* + T_{3x}^*\right) \\
F_5^* &= -m_1 q_1(a_{3z} - a_{1z}) - m_2 q_2 C_3(a_{3z} - a_{2z}) - \left(M_{1y}^* + M_{2y}^* + M_{3y}^*\right) \\
F_6^* &= m_1 q_1(a_{3y} - a_{1y}) + m_2 q_2 C_3(a_{3y} - a_{2y}) + m_2 q_2 S_3(a_{3x} - a_{2x}) - \left(T_{1z}^* + T_{2z}^* + T_{3z}^*\right) \\
F_7^* &= -T_{1x}^*,\ F_8^* = -T_{1y}^*,\ F_9^* = -T_{1z}^*,\ F_{10}^* = -T_{2x}^*,\ F_{11}^* = -T_{2y}^*,\ F_{12}^* = -T_{2z}^* \\
F_{13}^* &= -T_{3x}^*,\ F_{14}^* = -T_{3y}^*,\ F_{15}^* = -T_{3z}^*
\end{aligned}
\tag{11}
$$

Here,

$$
a_1 = \begin{bmatrix} \dot{\eta}_1 - q_1 \eta_5^2 - q_1 \eta_6^2 \\ q_1 \dot{\eta}_6 + 2\eta_1 \eta_6 + q_1 \eta_4 \eta_5 \\ -q_1 \dot{\eta}_5 - 2\eta_1 \eta_5 + q_1 \eta_4 \eta_6 \end{bmatrix}
$$

$$
a_2 = \begin{bmatrix} 2\eta_6(\eta_2 S_3 + q_2 \eta_3 C_3) - q_2 \eta_5(\eta_5 C_3 + \eta_4 S_3) + \dot{\eta}_2 C_3 + q_2 S_3(\dot{\eta}_6 - \dot{\eta}_3) - 2\eta_2 \eta_3 S_3 - q_2 C_3(\eta_3^2 + \eta_6^2) \\ 2\eta_6(\eta_2 C_3 - q_2 \eta_3 S_3) + q_2 \eta_4(\eta_5 C_3 + \eta_4 S_3) - \dot{\eta}_2 S_3 + q_2 C_3(\dot{\eta}_6 - \dot{\eta}_3) - 2\eta_2 \eta_3 C_3 + q_2 S_3(\eta_3^2 + \eta_6^2) \\ -2\eta_5(\eta_2 C_3 - q_2 \eta_3 S_3) - 2\eta_4(\eta_2 S_3 + q_2 \eta_3 C_3) - q_2(\dot{\eta}_5 C_3 + \dot{\eta}_4 S_3) + q_2 \eta_6(\eta_4 C_3 - \eta_5 S_3) \end{bmatrix}
$$

$$
a_3 = -\frac{m_1}{m_3} a_1 - \frac{m_2}{m_3} a_2
$$

$$
T_1^* = -J_1 \begin{bmatrix} \dot{\eta}_4 + \dot{\eta}_7 \\ \dot{\eta}_5 + \dot{\eta}_8 \\ \dot{\eta}_6 + \dot{\eta}_9 \end{bmatrix},\
T_2^* = -J_2 \begin{bmatrix} \dot{\eta}_4 + \dot{\eta}_{10} \\ \dot{\eta}_5 + \dot{\eta}_{11} \\ \dot{\eta}_6 + \dot{\eta}_{12} \end{bmatrix},\
T_3^* = -J_3 \begin{bmatrix} \dot{\eta}_4 + \dot{\eta}_{13} \\ \dot{\eta}_5 + \dot{\eta}_{14} \\ \dot{\eta}_6 + \dot{\eta}_{15} \end{bmatrix}
$$

Since spacecraft 1 and 2 are affected by the control force/torque, the actuator-failure spacecraft is not affected by other external forces except the gravitational force. Therefore, the generalized active force can be expressed as:

$$
\begin{aligned}
F_1 &= F_{1x}^g + F_{1x}^u - m_1/m_3 F_{3x}^g \\
F_2 &= C_3\left(F_{2x}^g + F_{2x}^u\right) - C_3 m_2/m_3 F_{3x}^g - S_3\left(F_{2y}^g + F_{2y}^u\right) + S_3 m_2/m_3 F_{3y}^g \\
F_3 &= q_2 C_3 m_2/m_3 F_{3y}^g - q_2 C_3\left(F_{2y}^g + F_{2y}^u\right) - q_2 S_3\left(F_{2x}^g - F_{2x}^u\right) + q_2 S_3 m_2/m_3 F_{3x}^g \\
F_4 &= -q_2 S_3\left(F_{2z}^g + F_{2z}^u\right) + q_2 S_3 m_2/m_3 F_{3z}^g + \left(\tau_{1x}^u + \tau_{2x}^u\right) \\
F_5 &= -q_1\left(F_{1z}^g + F_{1z}^u\right) + q_1 m_1/m_3 F_{3z}^g - q_2 C_3\left(F_{2z}^g + F_{2z}^u\right) + q_2 C_3 m_2/m_3 F_{3z}^g + \left(\tau_{1y}^u + \tau_{2y}^u\right) \\
F_6 &= q_1\left(F_{1y}^g + F_{1y}^u\right) - q_1 m_1/m_3 F_{3y}^g + q_2 C_3\left(F_{2y}^g + F_{2y}^u\right) - q_2 C_3 m_2/m_3 F_{3y}^g \\
&\quad + q_2 S_3\left(F_{2x}^g + F_{2x}^u\right) - q_2 S_3 m_2/m_3 F_{3x}^g + \left(\tau_{1z}^u + \tau_{2z}^u\right) \\
F_7 &= \tau_{1x}^u + \tau_{1x}^d,\ F_8 = \tau_{1y}^u + \tau_{1y}^d,\ F_9 = \tau_{1z}^u + \tau_{1z}^d,\ F_{10} = \tau_{2x}^u + \tau_{2x}^d,\ F_{11} = \tau_{2y}^u + \tau_{2y}^d,\ F_{12} = \tau_{2z}^u + \tau_{2z}^d \\
F_{13} &= \tau_{3x}^d,\ F_{14} = \tau_{3y}^d,\ F_{15} = \tau_{3z}^d
\end{aligned}
\tag{12}
$$

Here, F_i^g is the gravitational force, F_i^u is the control force, F_i^d is the disturbance force, τ_i^u is the control torque, τ_i^d is disturbance torque, and $F_i^g = -\mu m_i r_i/r_i^3 = -\mu m_i\left(r_f + \rho_i\right)/r_i^3$.

Based on the Kane equation, the multi-spacecraft formation dynamics equation can be expressed as follows:

$$
F_r^* + F_r = 0 \quad (r = 1, \cdots, 15)
\tag{13}
$$

The derivatives of generalized coordinates and generalized rates with respect to time are derived from Equations (9) and (13), as follows:

$$
\left\{
\begin{array}{l}
\dot{q}_1 = \eta_1, \dot{q}_2 = \eta_2, \dot{q}_3 = \eta_3 \\
\dot{q}_4 = (C_6\eta_5 - S_6\eta_6)/C_5 - nS_4T_5, \dot{q}_5 = S_6\eta_5 + C_6\eta_6 - nc_4, \dot{q}_6 = \eta_4 - (C_6\eta_5 - S_6\eta_6)T_5 + nS_4/C_5 \\
\dot{q}_7 = -(C_7\eta_7 + S_7\eta_8)T_8 - \eta_9, \dot{q}_8 = S_7\eta_7 - C_7\eta_8, \dot{q}_9 = -(C_7\eta_7 + S_7\eta_8)/C_8 \\
\dot{q}_{10} = -(C_{10}\eta_{10} + S_{10}\eta_{11})T_{11} - \eta_{12}, \dot{q}_{11} = S_{10}\eta_{10} - C_{10}\eta_{11}, \dot{q}_{12} = -(C_{10}\eta_{10} + S_{10}\eta_{11})/C_{11} \\
\dot{q}_{13} = -(C_{13}\eta_{13} + S_{13}\eta_{14})T_{14} - \eta_{15}, \dot{q}_{14} = S_{13}\eta_{13} - C_{13}\eta_{14}, \dot{q}_{15} = -(C_{13}\eta_{13} + S_{13}\eta_{14})/C_{14}
\end{array}
\right. \tag{14}
$$

$$
\left\{
\begin{array}{l}
\dot{\eta}_1 = q_1(\eta_5^2 + \eta_6^2) + \left(f_{1x} - \frac{1}{M}\sum_{i=1}^{3} m_i f_{ix}\right) \\[2mm]
\dot{\eta}_2 = q_2(\eta_3 - \eta_6)^2 + q_2(\eta_4 S_3 + \eta_5 C_3)^2 + C_3\left(f_{2x} - \frac{1}{M}\sum_{i=1}^{3} m_i f_{ix}\right) - S_3\left(f_{2y} - \frac{1}{M}\sum_{i=1}^{3} m_i f_{iy}\right) \\[2mm]
\dot{\eta}_3 = (\eta_4 S_3 + \eta_5 C_3)(\eta_4 C_3 - \eta_5 S_3) - \eta_4\eta_5 + \frac{2\eta_2(\eta_6 - \eta_3)}{q_2} - \frac{2\eta_1\eta_6}{q_1} \\[2mm]
\qquad + \frac{1}{q_1}\left(f_{1y} - \frac{1}{M}\sum_{i=1}^{3} m_i f_{iy}\right) - \frac{1}{q_2}\left[S_3\left(f_{2x} - \frac{1}{M}\sum_{i=1}^{3} m_i f_{ix}\right) + C_3\left(f_{2y} - \frac{1}{M}\sum_{i=1}^{3} m_i f_{iy}\right)\right] \\[2mm]
\dot{\eta}_4 = 2\frac{C_3}{S_3}\eta_5\left(\frac{\eta_1}{q_1} - \frac{\eta_2}{q_2}\right) + 2\eta_5\eta_3 - \frac{2\eta_4\eta_2}{q_2} - \frac{2\eta_4\eta_3 C_3}{S_3} - \eta_6\eta_5 \\[2mm]
\qquad - \frac{1}{q_2 S_3}\left(f_{2z} - \frac{1}{M}\sum_{i=1}^{3} m_i f_{iz}\right) + \frac{C_3}{q_1 S_3}\left(f_{1z} - \frac{1}{M}\sum_{i=1}^{3} m_i f_{iz}\right) \\[2mm]
\dot{\eta}_5 = -\frac{1}{q_1}\left(2\eta_1\eta_5 - q_1\eta_4\eta_6 + f_{1z} - \frac{1}{M}\sum_{i=1}^{3} m_i f_{iz}\right) \\[2mm]
\dot{\eta}_6 = -\frac{1}{q_1}\left(2\eta_1\eta_6 + q_1\eta_4\eta_5 - f_{1y} + \frac{1}{M}\sum_{i=1}^{3} m_i f_{iy}\right) \\[2mm]
\dot{\eta}_7 = \left(\tau_{1x}^u + \tau_{1x}^d\right)/J_1 - \dot{\eta}_4, \dot{\eta}_8 = \left(\tau_{1y}^u + \tau_{1y}^d\right)/J_1 - \dot{\eta}_5, \dot{\eta}_9 = \left(\tau_{1z}^u + \tau_{1z}^d\right)/J_1 - \dot{\eta}_6 \\[2mm]
\dot{\eta}_{10} = \left(\tau_{2x}^u + \tau_{2x}^d\right)/J_2 - \dot{\eta}_4, \dot{\eta}_{11} = \left(\tau_{2y}^u + \tau_{2y}^d\right)/J_2 - \dot{\eta}_5, \dot{\eta}_{12} = \left(\tau_{2z}^u + \tau_{2z}^d\right)/J_2 - \dot{\eta}_6 \\[2mm]
\dot{\eta}_{13} = \tau_{3x}^d/J_3 - \dot{\eta}_4, \dot{\eta}_{14} = \tau_{3y}^d/J_3 - \dot{\eta}_5, \dot{\eta}_{15} = \tau_{3z}^d/J_3 - \dot{\eta}_6
\end{array}
\right. \tag{15}
$$

Here,

$$
f_i = f_i^g + f_i^u + f_i^d, \ M = m_1 + m_2 + m_3,
$$

$$
\sum_{i=1}^{3} m_i f_i = -\mu r_{cm}\left(\frac{m_1}{r_1^3} + \frac{m_2}{r_2^3} + \frac{m_3}{r_3^3}\right) - \mu\left(\frac{m_1}{r_1^3}\rho_1 + \frac{m_2}{r_2^3}\rho_2 + \frac{m_3}{r_3^3}\rho_3\right) + m_1 f_1^u + m_2 f_2^u + F_1^d + F_2^d + F_3^d
$$

Equations (14) and (15) are the multi-spacecraft formation 6DOF coupled dynamics model for the actuator-failure spacecraft. It can be seen from this model that, in addition to the nonlinear terms brought by trigonometric functions, the dynamic model also reflects the interaction between the attitude and orbit. Therefore, this model takes into account the interaction between configuration changes and the relative attitude of the spacecraft. The nonlinear dynamic equation (15) can be regarded as a function of generalized coordinates q, generalized velocity η, and control variables u_c.

In this paper, only spacecraft 1 and 2 are controllable. The control variables are defined as $u_c = \begin{bmatrix} F_1^u & F_2^u & \tau_1^u & \tau_2^u \end{bmatrix}^{\mathrm{T}}$, and the state variables are defined as $g = \begin{bmatrix} q & \eta \end{bmatrix}^{\mathrm{T}} = \begin{bmatrix} q_1 & \cdots & q_{12} & \eta_1 & \cdots & \eta_{12} \end{bmatrix}^{\mathrm{T}}$. Here, $\bar{q}$ and $\bar{\eta}$ are the nominal states. This paper focuses on solving the attitude-orbit coupling control problem of the formation system between two controllable spacecraft and an uncontrollable spacecraft. Our objective is to design an event-triggered attitude-orbit coupling controller to guarantee that the attitude and orbit can reach nominal states under the limited communication bandwidth and actuator failures.

3. Event-Triggered Attitude-Orbit Coupling Control

Equation (15) is a nonlinear dynamic system, which is difficult to synthesize. Thus, to facilitate the controller design, the nonlinear dynamic is linearized at operating points $\bar{q}, \bar{\eta}$ and $\bar{u}_c$, where $\bar{u}_c$ is the nominal control variable to be designed later.

Define the deviation of the nominal state as δq, $\delta \eta$, δu_c. Considering the short-period small disturbance assumption near the nominal state, variables can be expressed as

$$q = \bar{q} + \delta q, \ \eta = \bar{\eta} + \delta \eta, \ u_c = \bar{u}_c + \delta u_c \qquad (16)$$

As a first-order Taylor expansion is performed at the nominal state, the state variable can be expressed as

$$\dot{g}(q, \eta, u_c) = \begin{bmatrix} \dot{q}_1 & \cdots & \dot{q}_{12} & \dot{\eta}_1 & \cdots & \dot{\eta}_{12} \end{bmatrix}^T$$
$$\approx g(\bar{q}, \bar{\eta}, \bar{u}_c) + \frac{\partial g}{\partial q}\Big|_{(\bar{q}, \bar{\eta}, \bar{u}_c)} \cdot \delta q + \frac{\partial g}{\partial \eta}\Big|_{(\bar{q}, \bar{\eta}, \bar{u}_c)} \cdot \delta \eta + \frac{\partial g}{\partial u_c}\Big|_{(\bar{q}, \bar{\eta}, \bar{u}_c)} \cdot \delta u_c \qquad (17)$$

After linearization, it can be expressed as

$$\delta \dot{g} = \begin{bmatrix} \delta \dot{q} \\ \delta \dot{\eta} \end{bmatrix} = A(\bar{q}, \bar{\eta}, \bar{u}_c) \begin{bmatrix} \delta q \\ \delta \eta \end{bmatrix} + B(\bar{q}, \bar{\eta}, \bar{u}_c) \delta u_c \qquad (18)$$

Here, $A(\bar{q}, \bar{\eta}, \bar{u}_c)$ is the state matrix, $B(\bar{q}, \bar{\eta}, \bar{u}_c)$ is the input matrix, and the specific forms are

$$A(\bar{q}, \bar{\eta}, \bar{u}_c) = \begin{bmatrix} \frac{\partial \dot{q}_1}{\partial q_1} & \cdots & \frac{\partial \dot{q}_1}{\partial q_{12}} & \frac{\partial \dot{q}_1}{\partial \eta_1} & \cdots & \frac{\partial \dot{q}_1}{\partial \eta_{12}} \\ \vdots & \ddots & \vdots & \vdots & \ddots & \vdots \\ \frac{\partial \dot{q}_{12}}{\partial q_1} & \cdots & \frac{\partial \dot{q}_{12}}{\partial q_{12}} & \frac{\partial \dot{q}_{12}}{\partial \eta_1} & \cdots & \frac{\partial \dot{q}_{12}}{\partial u_{12}} \\ \frac{\partial \dot{\eta}_1}{\partial q_1} & \cdots & \frac{\partial \dot{\eta}_1}{\partial q_{12}} & \frac{\partial \dot{\eta}_1}{\partial \eta_1} & \cdots & \frac{\partial \dot{\eta}_1}{\partial \eta_{12}} \\ \vdots & \ddots & \vdots & \vdots & \ddots & \vdots \\ \frac{\partial \dot{\eta}_{12}}{\partial q_1} & \cdots & \frac{\partial \dot{\eta}_{12}}{\partial q_{12}} & \frac{\partial \dot{\eta}_{12}}{\partial \eta_1} & \cdots & \frac{\partial \dot{\eta}_{12}}{\partial \eta_{12}} \end{bmatrix}_{(\bar{q}, \bar{\eta}, \bar{u}_c)}$$

$$B(\bar{q}, \bar{\eta}, \bar{u}_c) = \begin{bmatrix} \frac{\partial \dot{q}_1}{\partial u_{c1}} & \cdots & \frac{\partial \dot{q}_1}{\partial u_{c12}} \\ \vdots & \ddots & \vdots \\ \frac{\partial \dot{q}_{12}}{\partial u_{c1}} & \cdots & \frac{\partial \dot{q}_{12}}{\partial u_{c12}} \\ \frac{\partial \dot{\eta}_1}{\partial u_{c1}} & \cdots & \frac{\partial \dot{\eta}_1}{\partial u_{c12}} \\ \vdots & \ddots & \vdots \\ \frac{\partial \dot{\eta}_{12}}{\partial u_{c1}} & \cdots & \frac{\partial \dot{\eta}_{12}}{\partial u_{c12}} \end{bmatrix}_{(\bar{q}, \bar{\eta}, \bar{u}_c)}$$

To simplify the description, A is used to denote $A(\bar{q}, \bar{\eta}, \bar{u}_c)$ and B is used to denote $B(\bar{q}, \bar{\eta}, \bar{u}_c)$. The state equation of (18) is rewritten as:

$$\dot{X} = AX + Bu, \ X(0) = X_0, \ t \geq 0 \qquad (19)$$

Here, X is an n-dimensional state, u is a p-dimensional control input. A and B are constant-valued matrices of $n \times n$ and $n \times p$.

Considering the attitude-orbit coupling control system (19) of the multi-spacecraft formation, when $\dot{q} = 0$ and $\dot{\eta} = 0$, the configuration and relative attitude of the formation are stable. Multi-spacecraft attitude-orbit coupling control is composed of two parts: nominal control and deviation control. In order to achieve the desired configuration and relative attitude, it is assumed that the generalized coordinate nominal state is $\bar{q}$. Combining $\bar{q}$, $\dot{q} = 0$ and Equation (9), the generalized rate nominal state $\bar{\eta}$ is further obtained. Considering the nominal state $\bar{q}$ and $\bar{\eta}$, with $\dot{\eta} = 0$ and Equation (15), the control quantity $\bar{u}_c$ can be obtained.

When considering the actuator attenuation, the object model of the infinite time LQ problem can be expressed as:

$$\begin{cases} \dot{X} = AX + B\rho u, \ X(0) = X_0, t \in [0, \infty) \\ \quad J(u) = \int_0^\infty \left(X^{\mathrm{T}} QX + u^{\mathrm{T}} Ru \right) \mathrm{d}t \end{cases} \tag{20}$$

Here, $\rho = diag\{\rho_1, \rho_2, \ldots, \rho_n\}$ is an active factor of the actuator, satisfying $0 < \underline{\rho}_i \le \rho_i \le \bar{\rho}_i \le 1$, where $\underline{\rho}_i$ and $\bar{\rho}_i$ are constants; $\bar{\rho} = \max\{\bar{\rho}_i\}$ means the maximum value of $\bar{\rho}_i$; $\underline{\rho} = \min\left\{\underline{\rho}_i\right\}$ means the minimum value of $\underline{\rho}_i$, $i = 1, 2, \cdots, 6$.

Normally, the optimal $u(t)$ can be expressed as:

$$u(t) = KX(t), K = -R^{-1}B^{\mathrm{T}}P \tag{21}$$

Here, matrix P is the solution of the following matrix, the Riccati equation

$$PA + A^{\mathrm{T}}P + Q - \bar{\rho}PBR^{-1}B^{\mathrm{T}}P = 0 \tag{22}$$

Here, $\bar{\rho} = \max\{\bar{\rho}_i\}, i = 1, 2, \cdots, n$.

Since the calculation resources and communication bandwidth on orbit are limited, to save the calculation resources and reduce the burden of communication of the network, the event-trigger mechanism is introduced. However, the event trigger mechanism will cause signal transmission errors. If the control policies and event trigger mechanisms are designed independently, it may result in a decrease in control performance or even an unstable system. Therefore, event-triggering mechanisms and control strategies need to be jointly designed. In this section, the event-triggered control law and event-triggered mechanism will be co-designed.

According to (21), the event-trigger control law based on the LQR method can be rewritten as

$$u(t) = KX(t_k), \ t \in [t_k, t_{k+1}) \tag{23}$$

Here, $X(t_k)$ is the latest updated state vector. $\{t_k\}, k \in N$ is a non-periodic sampling series.

To adjust the event-triggered mechanism, the following dynamic event-triggered mechanism is designed:

$$\eta(t) + \beta(\sigma \left|\left| X(t) \right|\right|_2 - \kappa \left|\left| E(t) \right|\right|_2 + \mu e^{-\lambda t}) < 0 \tag{24}$$

Here, $E(t) = X(t_k) - X(t)$, $\beta > 0$, $\sigma > 0$, $\kappa > 0$, $\mu > 0$ and $\lambda > 0$ are positive parameters. $\eta(t)$ is a dynamic variable, which is defined as follows

$$\dot{\eta}(t) = -\alpha\eta(t) + (\sigma \left|\left| X(t) \right|\right|_2 - \kappa \left|\left| E(t) \right|\right|_2 + \mu e^{-\lambda t}) \tag{25}$$

Here, $\alpha > 0$ is a positive parameter. The initial condition of $\eta(t)$ is defined as $\eta(0) = \eta_0 > 0$.

Remark 1. *Compared with the sampling control, the control period of the sampling control is fixed, while the control period of the dynamic event-triggered control is variable.*

Remark 2. *Compared with the event-triggered control (etc.), the parameters of the event-triggered mechanism are constants, while the parameters of the dynamic event-triggered mechanism can be adaptively adjusted and thus may reduce the triggered times significantly. Moreover, it can be known that when* $\lim\limits_{t\to\infty} \eta(t) = 0$ *and* $\lim\limits_{t\to\infty} \mu e^{-\lambda t} = 0$, *the dynamic event-triggered condition*

$\eta(t) + \beta(\sigma||X(t)||_2 - \kappa||E(t)||_2 + \mu e^{-\lambda t}) < 0$ *will reduce to the static event-triggered condition* $\sigma||X(t)||_2 - \kappa||E(t)||_2 < 0$.

Lemma 1. *Given positive parameters β, σ, κ, μ, λ, α and η_0, then $\eta(t) \geq 0$ and $\forall t \in [t_k, t_{k+1})$ always hold.*

Proof. Considering the dynamic event-triggered mechanism (24), it can be known that $\forall t \in [t_k, t_{k+1})$, $\eta(t) + \beta(\sigma||X(t)||_2 - \kappa||E(t)||_2 + \mu e^{-\lambda t}) \geq 0$ holds. Since $\beta > 0$, we have $\beta(\sigma||X(t)||_2 - \kappa||E(t)||_2 + \mu e^{-\lambda t}) \geq (-1/\beta)\eta(t)$. From (28), it can be directly derived that $\dot{\eta}(t) \geq -(\alpha + 1/\beta)\eta(t)$, $\forall t \in [t_k, t_{k+1})$. By a comparison lemma, it can be concluded that the solution of $\eta(t)$ satisfies $\eta(t) \geq \hat{\eta}(t)$, where $\hat{\eta}(t)$ is the solution of equation $\dot{\hat{\eta}}(t) = -(\alpha + 1/\beta)\hat{\eta}(t)$ with $\hat{\eta}(0) = \eta_0$. Since $\hat{\eta}(t) = \eta_0 e^{-(\alpha+1/\beta)t} > 0$ and $\forall t \in [t_k, t_{k+1})$, we have $\eta(t) > 0$ and $\forall t \in [t_k, t_{k+1})$. The proof is completed. □

According to (20) and (23), (19) can be rewritten as

$$\dot{X} = AX + B\rho KX(t) + B\rho E(t) \tag{26}$$

Theorem 1. *Considering the attitude-orbit coupling control system (19) of a multi-spacecraft formation, the controller is designed as shown in Equation (23), where the state feedback matrix is obtained by Equation (22). The event-trigger condition is shown as in Equation (24). If there exists positive parameters β, σ, κ, μ, λ, α, γ and matrices B, P and K, the following conditions hold*

$$\begin{aligned} &\alpha\beta\sigma = \sigma + \gamma||PBB^T P|| \\ &\kappa > \gamma^{-1}\bar{\rho}^2||K^T K|| \\ &\alpha\beta\kappa = \kappa - \gamma^{-1}\bar{\rho}^2||K^T K|| \end{aligned} \tag{27}$$

Then the closed-loop control system is stable.

Proof. Consider the following Lyapunov function

$$V(t) = X^T(t)PX(t) + \eta(t) \tag{28}$$

Here, the P is the solution of Equation (22).
From (23), (25) and (26), one has

$$\begin{aligned} \dot{V}(t) = &X^T(t)(A^T P + PA)X(t) - X^T(t)PB\rho R^{-1}B^T PX(t) + 2X^T(t)PB\rho R^{-1} \\ &\times B^T PE(t) - \alpha\eta(t) + (\sigma||X(t)||_2 - \kappa||E(t)||_2 + \mu e^{-\lambda t}) \end{aligned} \tag{29}$$

Since there exists a positive parameter γ, the following inequality holds

$$2X^T(t)PB\rho KE(t) \leq \gamma||PBB^T P||\Big|\Big|X(t)\Big|\Big|_2 + \gamma^{-1}\Big|\Big|K^T \rho\rho K\Big|\Big|\Big|\Big|E(t)\Big|\Big|^2 \tag{30}$$

Thus, the Equation (33) can be rewritten as

$$\begin{aligned} \dot{V}(t) \leq &X^T(t)(A^T P + PA)X(t) - X^T(t)PB\rho R^{-1}B^T PX(t) \\ &+ \gamma||PBB^T P||||X(t)||_2 + \gamma^{-1}||K^T \rho\rho K||||E(t)||_2 - \alpha\eta(t) \\ &+ (\sigma||X(t)||_2 - \kappa||E(t)||_2 + \mu e^{-\lambda t}) \end{aligned} \tag{31}$$

Since the following inequality always holds

$$X^T(t)PB\rho R^{-1}B^T PX(t) - \bar{\rho}X^T(t)PBR^{-1}B^T PX(t) \leq 0 \tag{32}$$

according to (22), (31) and (32), one has

$$X^T(t)(A^TP + PA)X(t) - X^T(t)PB\rho R^{-1}B^TPX(t) \leq -X^T(t)QX(t) \tag{33}$$

Then, according to (22), (31) and (33), one has

$$\dot{V}(t) \leq -X^T(t)(Q + PB\rho R^{-1}B^TP)X(t) + \gamma||PBB^TP||\,||X(t)||_2 + \gamma^{-1}||K^T\rho\rho K||\,\Big|\Big|E(t)\Big|\Big|^2 \\ -\alpha\eta(t) + (\sigma||X(t)||_2 - \kappa||E(t)||_2 + \mu e^{-\lambda t}) \tag{34}$$

Define $Q_1 = Q + PB\underline{\rho}R^{-1}B^TP$ and $\underline{\rho} = \min\{\rho_i\}, i = 1, 2, \cdots, 6$. According to (27) and (34), one has

$$\dot{V}(t) \leq -X^T(t)Q_1X(t) - \alpha(\eta(t) - \beta(\sigma||X(t)||_2 - \kappa||E(t)||_2 + \mu e^{-\lambda t})) \tag{35}$$

According to Lemma 1, it can be known that $\forall t \in [t_k, t_{k+1})$,

$$\alpha(\eta(t) - \beta(\sigma||X(t)||_2 - \kappa||E(t)||_2 + \mu e^{-\lambda t})) > 0 \tag{36}$$

Hence, it can be concluded that $\forall t \in [t_k, t_{k+1})$, for $||X(t)|| \neq 0$, $\dot{V}(t) < 0$ holds, which means that the closed-loop system is stable. This completes the proof. □

In the following, we will focus on proving that the designed event-triggered mechanism has a nonzero upper bound, which shows that the Zeno behavior can be avoided.

Theorem 2. *Considering the attitude-orbit coupling control system (19) with controller (23), all conditions in Theorem 1 are assumed to be held. Then there exists a positive parameter $T_k > 0$, such that $t_{k+1} - t_k \geq T_k$ holds.*

Proof. Considering the system (19) and the control law (26), according to the definition of $E(t)$, it can be derived that:

$$\dot{E}(t) = \dot{X}(t) = AX(t) + B\rho KX(t_k) \tag{37}$$

Further, one has

$$\Big|\Big|\dot{E}(t)\Big|\Big| = \Big|\Big|A + B\rho K\Big|\Big|\,\Big|\Big|X(t_k)\Big|\Big| + \Big|\Big|A\Big|\Big|\,\Big|\Big|E(t)\Big|\Big| \tag{38}$$

As $E(t_k) = 0$, the solution to Equation (37) can be expressed as:

$$||E(t)|| \leq \frac{||A + B\rho K||\,||X(t_k)||}{||A||}(e^{||A||(t-t_k)} - 1) \tag{39}$$

In combination with the event-triggered condition (24), it can be derived that

$$\frac{1}{\beta\kappa}\sqrt{\eta(t) + \beta(\sigma||X(t)||_2 + \mu e^{-\lambda t})} \leq \frac{||A + B\rho K||\,||X(t_k)||}{||A||}(e^{||A||(t-t_k)} - 1) \tag{40}$$

Thus, one has

$$t - t_k \geq T_k = \frac{1}{||A||}\ln\left(1 + \frac{\vartheta_1}{\vartheta_2}\right) > 0 \tag{41}$$

Here, $\vartheta_1 = \frac{1}{\beta\kappa}\sqrt{\eta(t) + \beta(\sigma||X(t)||_2 + \mu e^{-\lambda t})}$ and $\vartheta_2 = \frac{||A+B\rho K||\,||X(t_k)||}{||A||}$, which means that the event-trigger mechanism designed in this paper can avoid the Zeno phenomena. This completes the proof. □

4. Simulations and Discussions

Aiming at a formation configuration composed of two controllable spacecrafts considering the control torque attenuation of actuators and one uncontrollable spacecraft with actuator failure, simulations of the attitude-orbit coupling closed-loop control of the multi-spacecraft formation, considering 6DOF relative attitude, were carried out.

Assume that the mass m_1, m_2 and the inertia I_1, I_2 of the controllable spacecraft 1 and spacecraft 2 are 500 kg and 150 kg·m^2. The mass m_3 of the uncontrollable spacecraft 3 is 2800 kg and the inertia of the uncontrollable spacecraft 3 is unknown.

The desired configuration of the three spacecrafts is an isosceles triangle with the uncontrollable spacecraft as the vertex, and the relative positional relationship is determined by Equation (1). It is expected that the configuration is symmetrically distributed about the y_f axis of the orbital system H. The relative attitude of each spacecraft is constant in the formation-fixed coordinate system B. The coefficients of the nominal state are shown in Tables 1–3.

Table 1. The relative position.

$\bar{\rho}_1$	$\bar{\rho}_2$	$\bar{\phi}$
12 m	12 m	120°

Table 2. The relative azimuth.

$\bar{\varphi}$	$\bar{\theta}$	$\bar{\psi}$
0°	0°	−30°

Table 3. The relative attitude angle.

$\bar{\alpha}_1$	$\bar{\beta}_1$	$\bar{\gamma}_1$	$\bar{\alpha}_2$	$\bar{\beta}_2$	$\bar{\gamma}_2$	$\bar{\alpha}_3$	$\bar{\beta}_3$	$\bar{\gamma}_3$
0°	0°	0°	0°	0°	0°	0°	0°	0°

Initial bias and process noise were added to the simulation. The error of the relative distance is (2.4 m, −2.4 m). The error of the relative distance change rate is (0.02 m/s, −0.03 m/s). The error of the configuration angle and the angle change rate is (−5°, 0.05°/s). The relative attitude-angle error of spacecraft 1 is (−6°, −5°, 3°), and the error of the attitude-angle change rate is (0.02°/s, 0.03°/s, −0.02°/s). The relative attitude-angle error of spacecraft 2 is (−4°, 6°, −3°). The error of the attitude-angle change rate is (−0.02°/s, −0.04°/s, 0.03°/s). Since the general relative attitude is the attitude relative to the orbit system, for the convenience of calculation, the relative azimuth/angle change rate is taken as 0.

The process noise includes the influence of the external disturbance force and disturbance torque. Considering the periodic change in the orbital motion, the process noise was designed as

$$
\begin{cases}
\boldsymbol{F}_1^d = \begin{bmatrix} 3 & 2 & 1.5 \end{bmatrix} \times 10^{-2} \sin(nt) \text{ N} \\
\boldsymbol{F}_2^d = \begin{bmatrix} 5 & 3 & -1 \end{bmatrix} \times 10^{-2} \sin(nt) \text{ N} \\
\boldsymbol{F}_3^d = \begin{bmatrix} 4 & -2 & -3 \end{bmatrix} \times 10^{-2} \sin(nt) \text{ N}
\end{cases}
$$
$$
\begin{cases}
\boldsymbol{\tau}_1^d = \begin{bmatrix} 2 & -1 & 1 \end{bmatrix} \times 10^{-4} \sin(nt) \text{ N} \cdot \text{m} \\
\boldsymbol{\tau}_2^d = \begin{bmatrix} 1 & 2 & -1 \end{bmatrix} \times 10^{-4} \sin(nt) \text{ N} \cdot \text{m}
\end{cases} \tag{42}
$$

The $\boldsymbol{Q}$, $\boldsymbol{R}$ were designed as follows:

$$
\begin{aligned}
\boldsymbol{Q} &= \text{diag}[100, 100, 100, 5, 5, 5, 100, 100, 100, 100, 100, 100, 1, 1, 1, 1, 1, 1, 1, 1, 1, 1, 1, 1] \\
\boldsymbol{R} &= \text{diag}\left[10, 10, 10, 10, 10, 10, 10^2, 10^2, 10^2, 10^2, 10^2, 10^2\right]
\end{aligned} \tag{43}
$$

$\rho_i, i = 1, 2, \cdots, 6$ represents the actuator effective factor for the attitude and orbit control. For the convenience of simulation, $\rho_i = 0.85 + 0.05 \sin(t)$ was set, so it can be known that $0.8 \leq \rho_i \leq 0.9$.

In order to reduce the communication frequency between the sensor and controller, the event trigger mechanism was introduced, which was designed as $||e(t)|| \leq 0.02||X(t)||$. The eigenvalue distribution of the open-loop system in the nominal state is shown in the left figure in Figure 2. From this figure, it can be seen that the open-loop system is unstable. After applying the event-triggered control law, the eigenvalue distribution of the closed-loop system is shown in the right graph in Figure 2, from which it can be seen that the closed-loop system is stable.
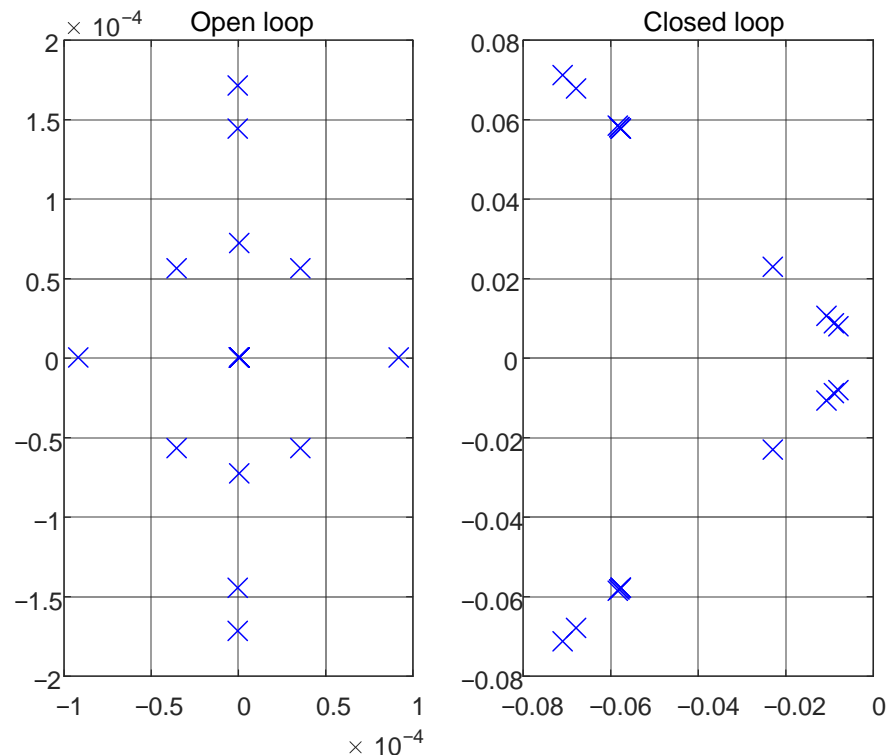
Figure 2. Eigenvalue distribution of open-loop and closed-loop systems.

The simulation results of the closed-loop system are shown in Figures 3–11. The simulation results show that the relative position and the attitude of each spacecraft can be quickly stabilized to the nominal state, so as to maintain the relative state of the six degrees of freedom of attitude orbit coupling of three-spacecrafts formation. The tracking error is small. Figures 3–5 demonstrate the curves of the relative distance, relative configuration angle and azimuth angle. It is also seen that the relative distance, relative configuration angle and the azimuth angle converge to a stable state at 100 s, 200 s and 300 s, respectively. It should be emphasized that the change process of the spatial configuration can be seen from Figure 6.
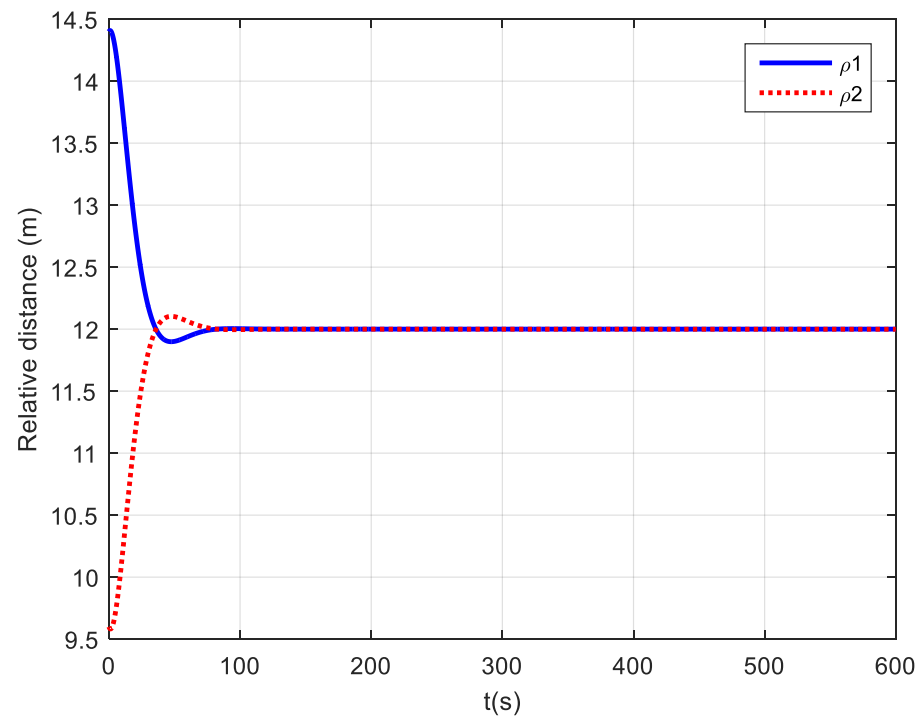
Figure 3. Relative distance curve.
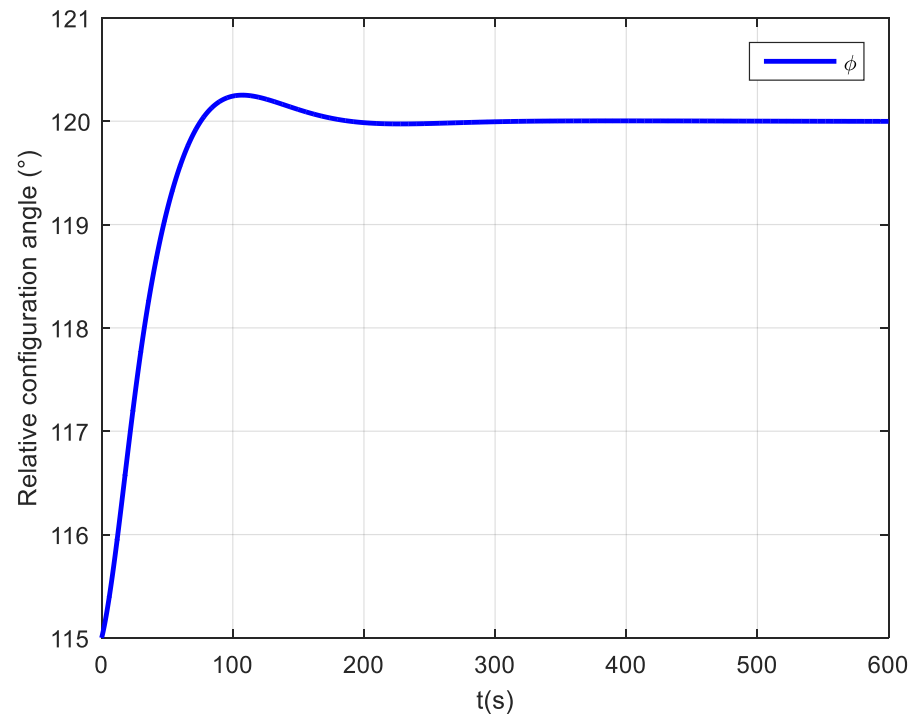
Figure 4. Relative configuration-angle curve.
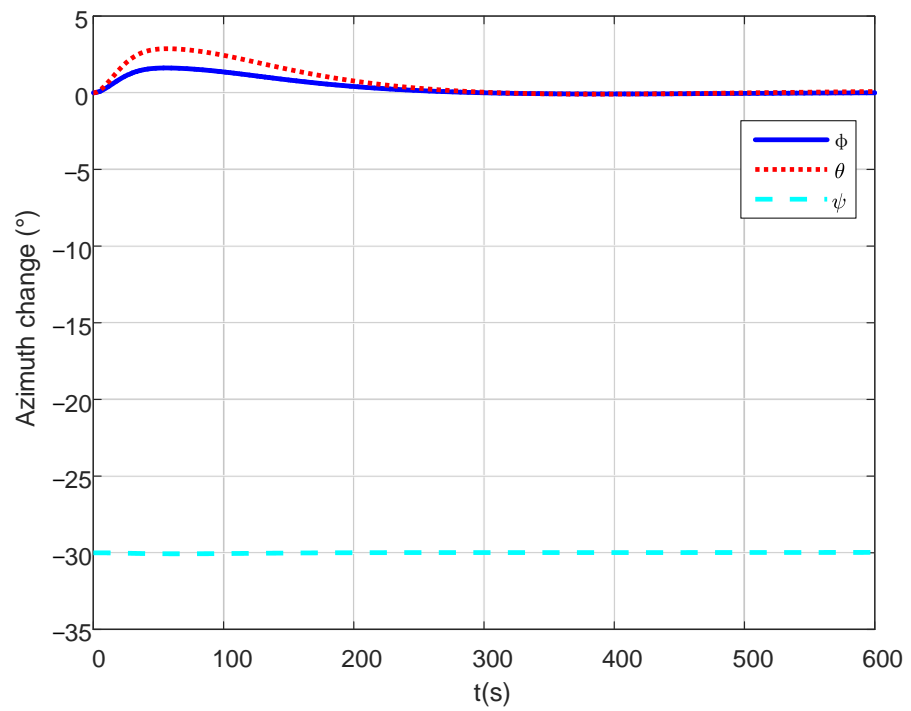
Figure 5. Azimuth angle-change curve.
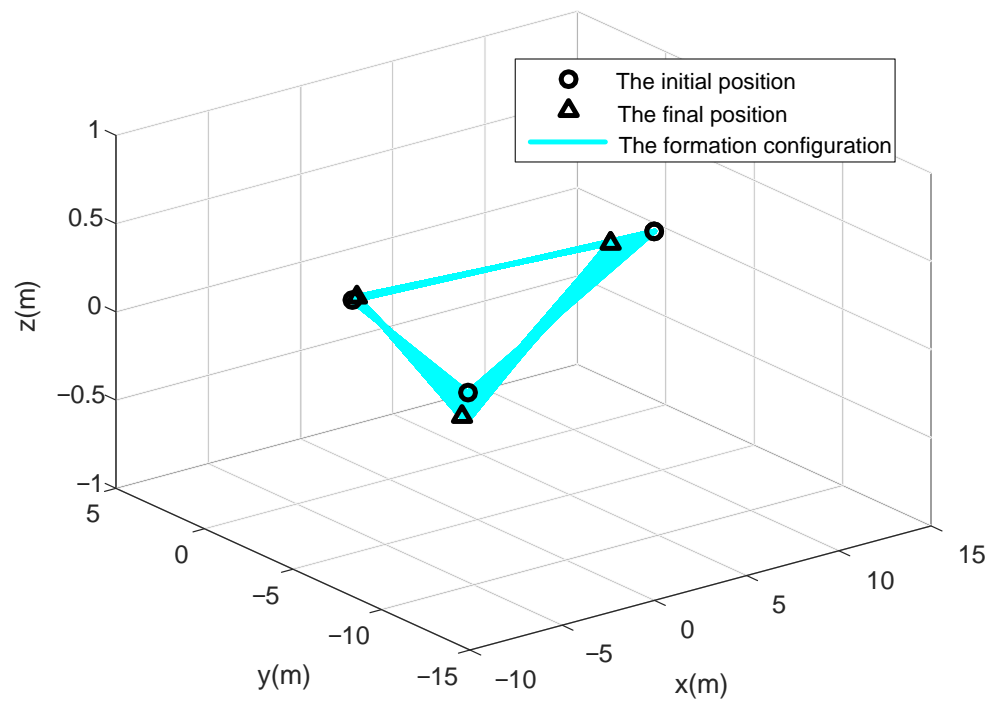
Figure 6. Formation-configuration change.
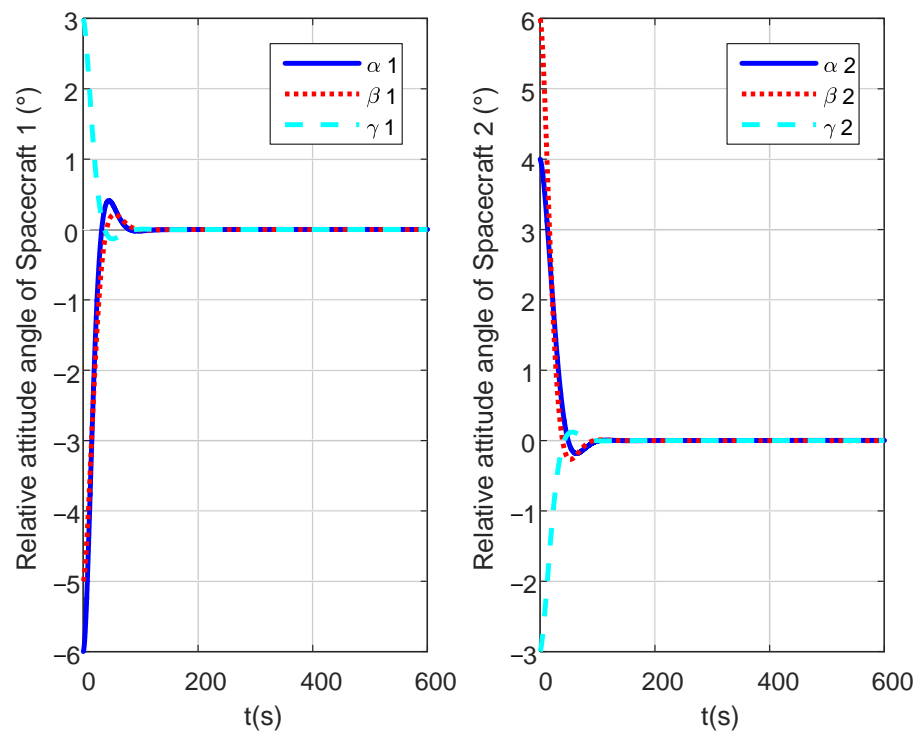
Figure 7. Relative attitude-angle chance curve.
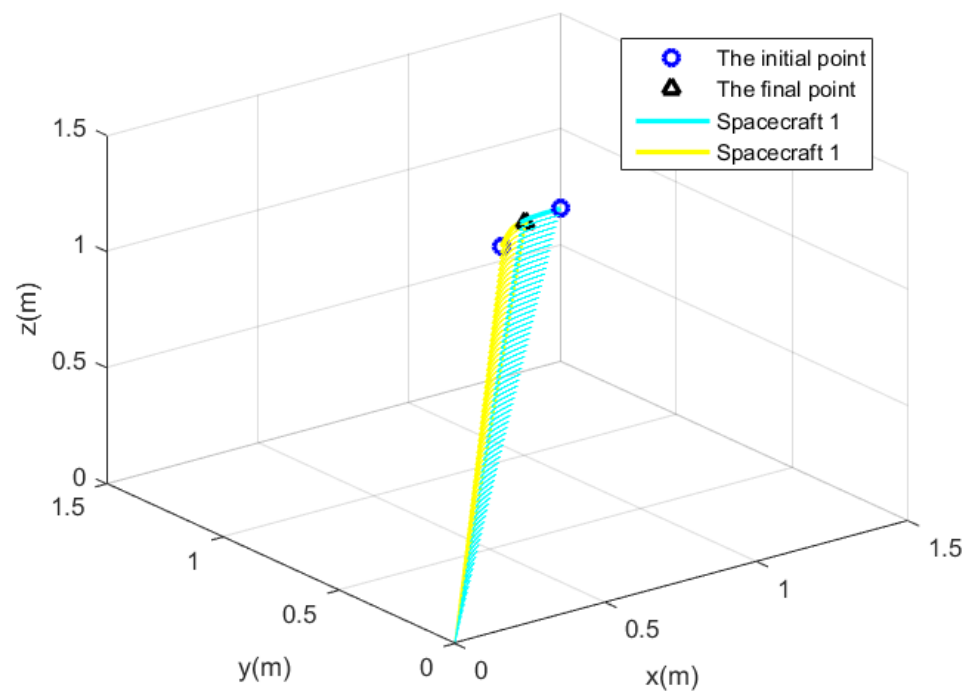
Figure 8. Changes in the direction of the relative attitude.
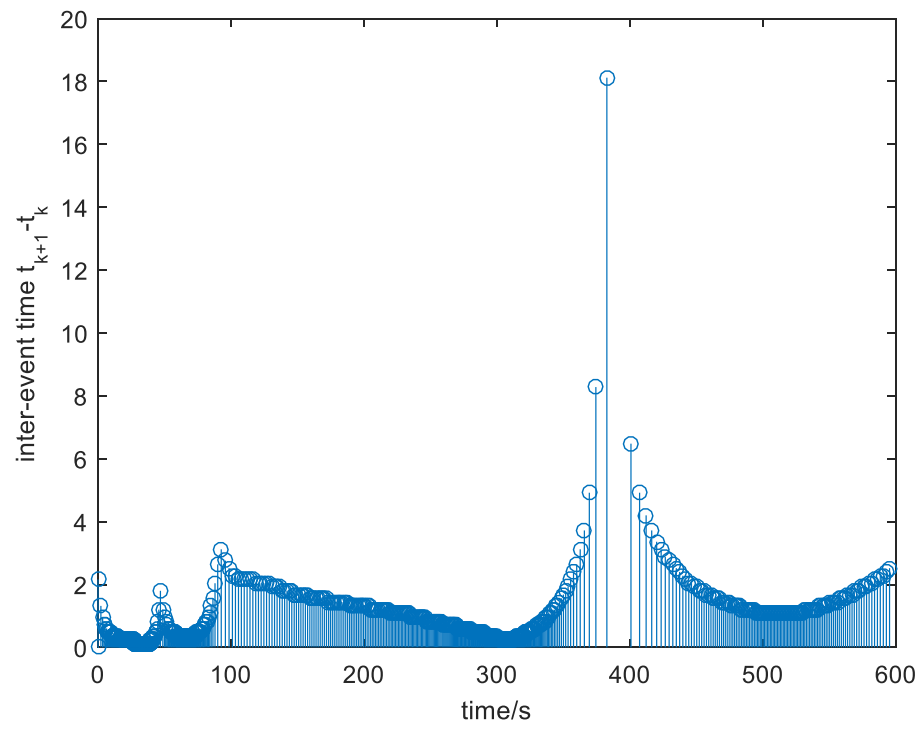
Figure 9. Time interval of event trigger.
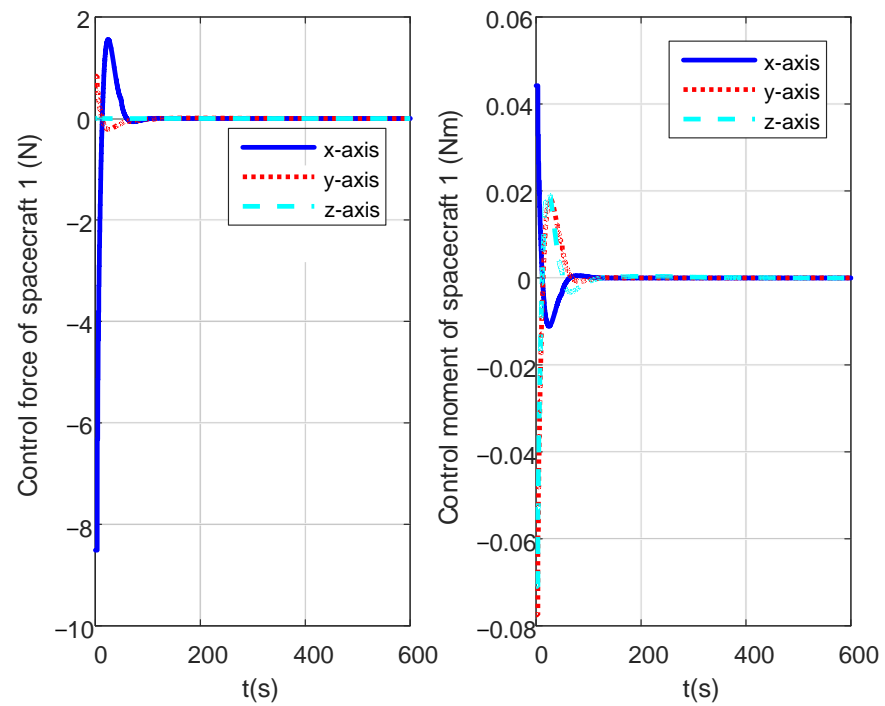
Figure 10. Control force and control moment of spacecraft 1.
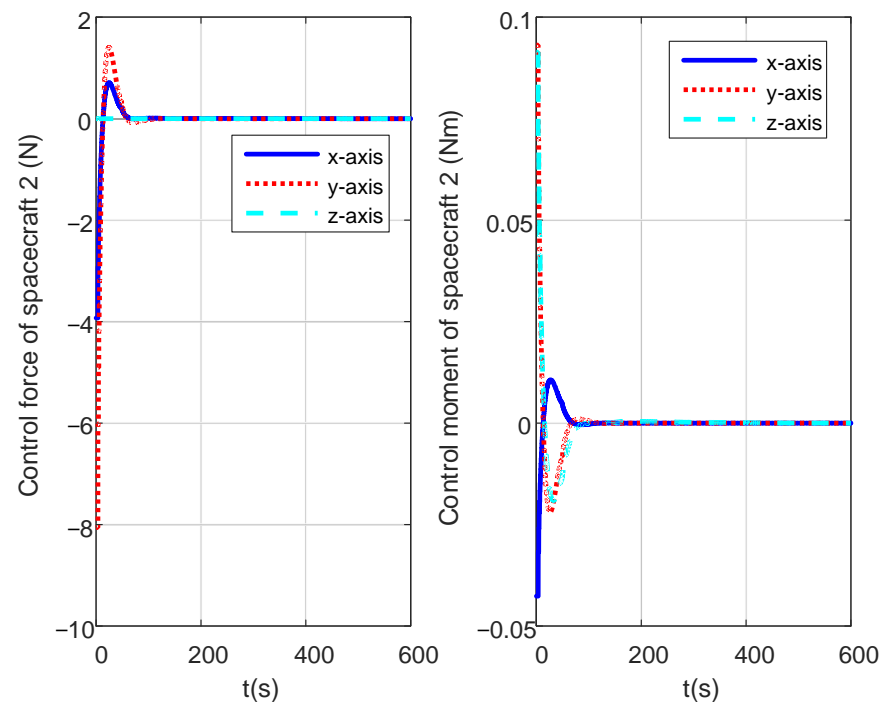
Figure 11. Control force and control moment of spacecraft 2.

From Figures 7 and 8, one can find the change in the relative attitude pointing of spacecraft 1 and 2 in the fixed-coordinate system of the formation system. The relative attitude pointing of spacecraft 1 and 2 tends to be consistent, which can complete the synchronous control of attitude pointing while realizing orbit adjustment. From Figure 7, the relative attitude angle of spacecraft 1 can be seen and spacecraft 1 is in a stable state at 100 s.

It can be seen from Figure 9 that the trigger time interval of any two events is greater than 0, of which the minimum value is 0.12 s and the maximum value is 18.12 s. At present, the sampling period in the project can be better than 0.064 s. Therefore, the minimum time interval of two event triggers is greater than the sampling period. This indicates that the designed event-trigger mechanism is effective. It can not only avoid the Zeno phenomenon, but also meet the requirements of practical engineering use. It can be seen from Figures 10 and 11 that the control force required by spacecraft 1 and spacecraft 2 is less than 9 N. The required control torque is less than 0.1 Nm. Therefore, the actual engineering capability can meet the demand.

5. Conclusions

In this paper, we have proposed an event-triggered attitude-orbit coupled control approach to solve the problem of the attitude-orbit coupled control system of a multi-spacecraft formation with limited communication capability and actuator failure. First, an integrated nonlinear dynamic model including the coupling characteristics of attitude and orbit is established based on the Kane equation. Second, the nonlinear dynamic model is linearized at the reference state to facilitate the controller design. In order to reduce the communication rate, the dynamic event-triggered mechanism was introduced. Finally, an event-triggered fault tolerant control law is developed to overcome the influence of actuator failure and the event-triggered mechanism. The stability of closed-loop control systems is analyzed. A sufficient condition that guarantees that Zeno's behavior can be avoided is given. Simulation results were given to show the effectiveness of the proposed method. Further research will focus on more complicated cases, such as partial state unmeasurable, signal quantization, torque distribution and optimization, unknown disturbances, and additive actuator faults, which were not addressed in this design work.

References

1. Gao, Z.F.; Wang, S. Fault estimation and fault tolerance control for spacecraft formation systems with actuator fault and saturation. *Optim. Control Appl. Meth.* **2021**, *42*, 1591–1611. [CrossRef]
2. Zou, A.M.; Kruishna, D.K. Robust attitude coordination control for spacecraft formation flying under actuator failures. *J. Guid. Control Dynam.* **2012**, *35*, 1247–1255. [CrossRef]
3. Gui, Y.; Jia, Q.X.; Li, H.Y.; Cheng, Y.H. Reconfigurable fault-tolerant control for spacecraft formation flying based on iterative learning algorithms. *Appl. Sci.* **2022**, *12*, 2485. [CrossRef]
4. Zhang, C.X.; Wang, J.H.; Zhang, D.X.; Shao, X.W. Fault-tolerant adaptive finite-time attitude synchronization and tracking control for multi-spacecraft formation. *Aerosp. Sci. Technol.* **2018**, *73*, 197–209. [CrossRef]
5. Li, J.Q.; Kumar, K.D. Decentralized fault-tolerant control for satellite attitude synchronization. *IEEE Trans. Fuzzy Syst.* **2012**, *20*, 572–585. [CrossRef]
6. Chen, G.J.; Chang, L.; Yang, X.B.; Yang, C.L.; Li, Y.B. Anti-disturbance and fault-tolerant control of dual-satellite formation configuration maintenance. *Opt. Precis. Eng.* **2021**, *29*, 605–615. [CrossRef]
7. Sun, L. Adaptive fault-tolerant constrained control of cooperative spacecraft rendezvous and docking. *IEEE Trans. Ind. Electron.* **2020**, *67*, 3107–3115. [CrossRef]
8. Gui, H.; de Ruiter, A.H.J. Adaptive fault-tolerant spacecraft pose tracking with control allocation. *IEEE Trans. Control. Syst. Technol.* **2019**, *27*, 479–494. [CrossRef]
9. Wang, P.K.C.; Hadaegh, F.Y. Coordination and control of multiple microspacecraft moving in formation. *J. Astronaut. Sci.* **1996**, *44*, 315–355.
10. Wang, P.K.C.; Hadaegh, F.Y.; Lau, K. Synchronized formation rotation and attitude control of multiple free-flying spacecraft. *J. Guid. Control Dynam.* **1999**, *22*, 28–35. [CrossRef]
11. Wang, J.Y.; Liang, H.Z.; Sun, Z.W. Finite-time control for spacecraft formation with dual-number-based description. *J. Guid. Control Dynam.* **2012**, *35*, 950–962. [CrossRef]
12. Sun, W.Z. 6-DOF robust adaptive terminal sliding mode control for spacecraft formation flying. *Acta Astronaut.* **2012**, *73*, 76–87.
13. Lee, D. Spacecraft coupled tracking maneuver using sliding mode control with input saturation. *J. Aerosp. Eng.* **2015**, *28*, 1–11. [CrossRef]
14. Daero, L.; Sanyal, A.; Eric, B. Asymptotic tracking control for spacecraft formation flying with decentralized collision avoidance. *J. Guid. Control Dynam.* **2014**, *2514*, 1–14.
15. Zhang, B.Q.; Song, S.M.; Chen, X.L. Decentralized robust coordinated control for formation flying spacecraft with coupled attitude and translational dynamics. *Proc. Inst. Mech. Eng. Part G J. Aerosp. Eng.* **2013**, *227*, 798–815. [CrossRef]
16. Kim, Y.; Ahn, C. Point targeting of multisatellites via a virtual structure formation flight scheme. *J. Guid. Control Dynam.* **2009**, *32*, 1330–1344.
17. Ren, W. Distributed cooperative attitude synchronization and tracking for multiple rigid bodies. *IEEE Trans. Control. Syst. Technol.* **2010**, *18*, 383. [CrossRef]
18. Zou, A.M. Attitude coordination control for a group of spacecraft without velocity measurements. *IEEE Trans. Control. Syst. Technol.* **2012**, *20*, 1160–1174.
19. Zou, A.M.; Ruiter, A.D.; Kumar, K.D. Distributed finite-time velocity-free attitude coordination control for spacecraft formations. *Automatica* **2016**, *67*, 46–53. [CrossRef]
20. Liu, R.X.; Cao, X.B.; Liu, M.; Zhu, Y. 6-DOF fixed-time adaptive tracking control for spacecraft formation flying with input quantization. *Inf. Sci.* **2019**, *475*, 82–99. [CrossRef]
21. Huan, H.; Zhu, Y.; Yang, L.; Zhang, Y. Stability and shape analysis of relative equilibrium for three-spacecraft electromagnetic formation. *Acta Astronaut.* **2014**, *94*, 116–131. [CrossRef]
22. Huan, H.; Yang, L.; Zhu, Y.; Zhang, Y. Dynamics and relative equilibrium of spacecraft formation with non-contacting internal forces. *J. Aerosp. Eng.* **2014**, *228*, 1171–1182.
23. Mishra, S.K.; Jha, A.V.; Verma, V.K.; Appasani, B.; Bizon, N. An optimized triggering algorithm for event-triggered control of networked control systems. *Mathematics* **2019**, *9*, 1262. [CrossRef]

24. Sarjaš, A.; Gleich, D. Toward embedded system resources relaxation based on the event-triggered feedback control approach. *Mathematics* **2022**, *10*, 550. [CrossRef]

25. Demirel, B.; Ghadimi, E.; Quevedo, D.E.; Johansson, M. Optimal control of linear systems with limited control actions: Threshold-based event-triggered control. *IEEE Trans. Control. Syst. Netw.* **2018**, *5*, 1275–1286. [CrossRef]

26. Qiu, J.B.; Sun, K.K.; Wang, T.; Gao, H.J. Observer-based fuzzy adaptive event-triggered control for pure-feedback nonlinear systems with prescribed performance. *IEEE Trans. Fuzzy Syst.* **2019**, *27*, 2152–2162. [CrossRef]

27. Li, X.; Sun, Z.; Tang, Y.; Karimi, H. Adaptive event-triggered consensus of multiagent systems on directed graphs. *IEEE Trans. Automat. Control* **2021**, *66*, 1670–1685. [CrossRef]

28. Qi, J.R.; Liao, H.; Xu, Y.F. Event-triggered attitude-tracking control for a cableless non-contact close-proximity formation satellite. *Aerospace* **2022**, *9*, 138. [CrossRef]

29. Xie, X.; Sheng, T.; He, L. Distributed attitude synchronization for spacecraft formation flying via event-triggered control. *Appl. Sci.* **2021**, *11*, 6299. [CrossRef]